792–803 *Nucleic Acids Research, 2018, Vol. 46, No. 2* *Published online 4 December 2017*
doi: 10.1093/nar/gkx1199

Improving CRISPR–Cas specificity with chemical modifications in single-guide RNAs

Daniel E. Ryan[1], David Taussig[1], Israel Steinfeld[1], Smruti M. Phadnis[1], Benjamin D. Lunstad[2], Madhurima Singh[1], Xuan Vuong[1], Kenji D. Okochi[2], Ryan McCaffrey[2], Magdalena Olesiak[3], Subhadeep Roy[2], Chong Wing Yung[1], Bo Curry[1], Jeffrey R. Sampson[1], Laurakay Bruhn[1,*] and Douglas J. Dellinger[2]

[1]Agilent Research Laboratories, Santa Clara, CA, USA, [2]Agilent Research Laboratories, Boulder, CO, USA and [3]University of Colorado, Boulder, CO, USA

Received September 22, 2017; Revised November 12, 2017; Editorial Decision November 15, 2017; Accepted November 17, 2017

ABSTRACT

CRISPR systems have emerged as transformative tools for altering genomes in living cells with unprecedented ease, inspiring keen interest in increasing their specificity for perfectly matched targets. We have developed a novel approach for improving specificity by incorporating chemical modifications in guide RNAs (gRNAs) at specific sites in their DNA recognition sequence ('guide sequence') and systematically evaluating their on-target and off-target activities in biochemical DNA cleavage assays and cell-based assays. Our results show that a chemical modification (2′-*O*-methyl-3′-phosphonoacetate, or 'MP') incorporated at select sites in the ribose-phosphate backbone of gRNAs can dramatically reduce off-target cleavage activities while maintaining high on-target performance, as demonstrated in clinically relevant genes. These findings reveal a unique method for enhancing specificity by chemically modifying the guide sequence in gRNAs. Our approach introduces a versatile tool for augmenting the performance of CRISPR systems for research, industrial and therapeutic applications.

INTRODUCTION

CRISPR–Cas systems evolved to function on relatively small genomes in bacteria, but the recent proliferation of applications in larger genomes has created a growing need for higher specificity (1–5), especially for applications such as therapeutics where off-target activities have the potential to introduce deleterious effects (6,7). Various approaches have been reported to increase the specificity of CRISPR–Cas9 to minimize off-target events (8). These include truncations (9) and extensions (10) at the 5′ ends of gRNAs, co-localization of paired nickase mutants of Cas9 (11), fusion of catalytically inactive dCas9 to dimerization-dependent Fok1 nuclease (12,13), and engineered higher-fidelity versions of Cas9 protein (14–16). Other approaches control the duration of CRISPR activity in eukaryotic cells, for example by transient delivery of Cas9 and gRNA as a ribonucleoprotein complex (gRNP) via cationic lipids or electroporation (17,18), by inducible temporal control (19,20), or by timed addition of a CRISPR–Cas9 inhibitor (21) and other strategies. Among these options, transient delivery of gRNP complex has gained widespread favor and the other methods have yet to be broadly adopted.

Here, we explore an alternative means of modulating the specificity of CRISPR–Cas systems by incorporating chemical modifications in the 20-nucleotide (nt) guide sequence at the 5′ end of a gRNA which mediates the specificity of Cas9 in recognizing and hybridizing complementary protospacers. We have developed robust synthetic chemistry methods to produce single-guide RNAs (sgRNAs) with high fidelity and purity (22) and have reported that certain chemical modifications in the first and last three terminal nucleotides of sgRNAs can substantially boost CRISPR–Cas9 indel rates and homology-directed repair (HDR) editing events (23). The terminal modifications are thought to provide resistance to exonucleases, which is especially helpful in primary cells. Other studies exploring the potential advantages of chemical modifications in gRNAs employed crRNA and tracrRNA strands in dual-guide RNA systems and showed that chemical modifications in the crRNA strand can boost indel frequencies in transfected human cells (24–26), can enable conjugation of donor DNA for template-directed repair (27), and reportedly can improve the targeting specificity of truncated crRNAs by extensive modification of their ribose-phosphate backbones with 2′-*O*-methine-4′ bridges, phosphorothioates, and 2′-fluoro substituents in specific combinations (24).

*To whom correspondence should be addressed. Tel: +1 408 553 2475; Email: laurakay_bruhn@agilent.com

© The Author(s) 2017. Published by Oxford University Press on behalf of Nucleic Acids Research.
This is an Open Access article distributed under the terms of the Creative Commons Attribution License (http://creativecommons.org/licenses/by-nc/4.0/), which permits non-commercial re-use, distribution, and reproduction in any medium, provided the original work is properly cited. For commercial re-use, please contact journals.permissions@oup.com

In the present work, we chemically synthesized sgRNAs in which we systematically walked individual MP modifications across the 20-nt guide sequence of sgRNAs targeting four different genes, and each sgRNA was complexed with *Streptococcus pyogenes* Cas9 protein to evaluate the gene editing specificity of the Cas9 sgRNP. Importantly, we identified specific positions in sgRNA guide sequences where MP modification improves cleavage specificity across a variety of target loci and cell types, in several instances improving specificity by an order-of-magnitude or greater while maintaining high on-target activity.

MATERIALS AND METHODS

sgRNA synthesis

RNA oligomers were synthesized on a Dr Oligo 48 synthesizer (Biolytic Lab Performance, Inc.) using 2′-*O*-thionocarbamate-protected nucleoside phosphoramidites (Sigma-Aldrich) on controlled pore glass (Prime Synthesis, Inc.) according to previously described procedures (22). 2′-*O*-Methyl phosphoramidites were purchased from Thermo Scientific, and incorporated into RNA oligomers under the same conditions as the 2′-*O*-thionocarbamate protected phosphoramidites. The 2′-*O*-methyl-5′-*O*-dimethoxytrityl-3′-*O*-(diisopropylamino)-phosphinoacetic acid 1,1-dimethyl-2-cyanoethyl ester nucleosides used for synthesis of MP- and MSP-modified RNAs were synthesized according to published methods (22,28). For phosphorothioate-containing oligomers, the iodine oxidation step after the coupling reaction was replaced by a sulfurization step using a 0.05 M solution of 3-((*N*,*N*-dimethylaminomethylidene)amino)-3*H*-1,2,4-dithiazole-5-thione in a pyridine–acetonitrile (3:2) mixture for 6 min. Unless otherwise noted, reagents for solid-phase RNA synthesis were purchased from Glen Research. All oligonucleotides were purified using reversed-phase high-performance liquid chromatography (HPLC) and analyzed by liquid chromatography–mass spectrometry (LC-MS) using an Agilent 1290 Infinity series LC system coupled to an Agilent 6545 Q-TOF (time-of-flight) mass spectrometer as described previously (23). In all cases the mass determined by deconvolution of the series of peaks comprising multiple charge states in a mass spectrum of purified sgRNA matched the expected mass. Supplementary Table S1 shows the sequences of all sgRNAs.

T_m measurements

Thermal denaturation studies were performed on an Agilent Cary 100 Bio UV-visible spectrophotometer equipped with a 6 × 6 multicell block Peltier cuvette holder and a thermoelectric temperature controller. Unmodified or modified RNA was mixed with complementary ssODN in a 1:1 molar ratio under conditions representing physiological salt concentrations (10 mM sodium phosphate, 130 mM NaCl pH 7.3) at a final duplex concentration of 1 μM. Samples were annealed by heating to 90°C for 5 min followed by slow cooling at 0.5 deg min^{-1} to 15°C. For the measurement, the instrument was programed to heat from 15 to 90°C at 0.2 deg min^{-1}. UV absorbance was monitored at 260 nm and recorded at 1 min intervals. Melting temperatures T_m (heating phase) and T_ms (cooling phase) were determined by the maximum of first derivative plots and averaged over multiple cycles.

Biochemical in vitro DNA cleavage (IVC) assays

Each PAM-addressable on- or off-target sequence was generated in a linearized 2.8-kb DNA fragment by preparative PCR amplification of plasmid-borne human sequence (IDT MiniGene™) as listed in the *GRChg38* reference genome. IVC assays were performed in a 10 μL reaction volume containing 25 fmoles of linearized DNA in the presence of 100 nM sgRNA, 60 nM recombinant Cas9 protein (Agilent), 50 mM Tris–HCl, 140 mM KCl, 10 mM NaCl, 0.8 mM $MgCl_2$ and 0.2 mM spermine at pH 7.5 by incubating at 37°C for 1 h. Upon completion, 0.5 μl of RNace-It (Agilent) was added, and incubation was continued at 37°C for 5 min followed by 70°C for 15 min. Aliquots were analyzed on D5000 ScreenTape using an Agilent 4200 TapeStation. Cleavage yields were calculated by the formula: $(a/b) \times 100$ where a is the sum of band intensities of both DNA fragments produced by Cas9 cleavage, and b is the sum of band intensities of cleaved and uncleaved DNA.

Cell culture and nucleofections

Human K562 cells were obtained from ATCC and were cultured in RPMI 1640 media supplemented with 10% bovine growth serum (Thermo Fisher). K562 cells (within passage number 3 to 9) were nucleofected using a Lonza 4D-Nucleofector (96-well Shuttle device, program FF-120) per manufacturer's instructions. Nucleofections utilized a Lonza SF Cell Line kit (V4SC-2960) with 0.2 million cells in 20 ul of media, 125 pmoles of sgRNA, 50 pmoles of recombinant Cas9 protein (Thermo Fisher), and optionally 100 pmoles of ssODN donor template. Cells were cultured at 37°C in ambient oxygen and 5% carbon dioxide and were harvested at 48 h post-transfection. Human iPSCs were maintained in E8 medium (Gibco) on growth factor–reduced matrigel (BD Biosciences) coated cell culture plates. Cells were nucleofected using the Lonza 4D-Nucleofector (program CB-150) with a P3 Primary Cell 4D-Nucleofector kit (V4SP-3096). Cells were harvested at 48 hr post-transfection. Mobilized human peripheral blood CD34-positive hematopoietic stem and progenitor cells (CD34+ HSPCs) were purchased from AllCells (Alameda, CA) and thawed per manufacturer's instructions. CD34+ HSPCs were maintained in X-VIVO 15 (Lonza) supplemented with SCF (100 ng/ml), TPO (100 ng/ml), and Flt3-Ligand (100 ng/ml). CD34+ HSPCs were nucleofected using the Lonza 4D-Nucleofector (program EO-100) with a P3 Primary Cell kit. Cells were harvested at 72 h post-transfection.

PCR-targeted deep sequencing to quantify efficiency and specificity of genome modifications

Genomic DNA was extracted from cultured transfected cells using a QIAcube HT with a QIAmp DNA Mini kit (Qiagen) per manufacturer's instructions. Approximately 1

μg of purified gDNA was used with Hot-Start Q5 2X Master Mix polymerase (NEB) and gene-specific primers (480 pM, IDT) to amplify on- and off-target loci of interest. The primers had extensions to add sequencing primer sites in the first stage of PCR (protocol: 98°C, 5 min; (98°C, 20 s; 60°C, 20 s; 72°C, 30 s) × 30 cycles; 72°C, 3 min). The gene-specific PCR products were combined for each gDNA sample, diluted 10-fold, and subjected to a second stage of PCR to attach sequencing adaptors (protocol: 98°C, 5 min; (98°C, 20 s; 61°C, 20 s; 72°C, 30 s) × 6 cycles; 72°C, 3 min). PCR products were combined into a single tube and purified using Agencourt AMPure XP beads (Beckman Coulter) per manufacturer's instructions. Library concentration was determined using a DNA 1000 Bioanalyzer (Agilent). Paired-end 2 × 250-bp reads were sequenced on a MiSeq (Illumina) at 10.4 pM along with 20.5% PhiX. The primer, index, and target sequences employed are listed in Supplementary Table S2.

SureSelect enrichment of on- and off-target loci for *HBB* targeting in K562 cells

An Agilent SureSelect library of baits was designed with overlapping sequence coverage to capture a 1-kb segment of genomic DNA centered on the on-target site in *HBB*, and 960 discrete potential off-target sites including all sequences in the human genome having five or fewer mismatches versus the 20-bp target sequence in *HBB* and which have an adjoining NGG or NAG PAM as required for Cas9 recognition. K562 cells were nucleofected with sgRNP in triplicate, and the cultured cells were harvested at 48 hr post-transfection. Genomic DNA was isolated and processed according to Agilent's SureSelect^{XT} HiSeq protocol at www.agilent.com/cs/library/usermanuals/Public/G7530--90000.pdf. SureSelect-captured genomic DNA fragments were sequenced on an Illumina HiSeq 4000 sequencer using Illumina reagents for paired-end 2 × 150-bp sequencing reads. The Illumina sequencing data were analyzed as described below to calculate indel frequencies.

Analysis of Illumina sequencing data

Mapping of reads to the human genome was performed using BWA-MEM (bwa-0.7.10) software set to default parameters. Reads yielding inconsistent paired-end mappings, low-quality mappings, or secondary alignments were discarded from the analysis. Also discarded were reads failing to map across a 40-bp window centered on the potential Cas9 cleavage site while allowing indels. Retained reads were scored as having an indel or not according to whether an insertion or deletion was found within 10 bp of the Cas9 cleavage site. Mapped reads were segregated according to on- or off-target locus and were binned by the presence or absence of an indel; the tally of reads per bin was used to calculate %indels formed at the on-target site and likewise at each off-target site. Indel frequencies and standard deviations were calculated using logit-transformed %indel yields, $\ln(r/(1-r))$ where r is a %indel yield, to closely approximate a normal distribution. Triplicate mock transfections provided a negative control, and samples with indel frequencies significantly higher (t-test $p < 0.05$) than the mock transfection (minus Cas9 sgRNP) were considered above background. The t-test was performed on logit-transformed indel frequencies. In a typical experiment, indel frequencies measured in mock transfections ranged from 0.02% to 0.09% (see Supplementary Table S4), suggesting a detection limit for true activity by Cas9 to be ∼0.05%.

Calculation of ON:OFF target cleavage ratios and specificity scores

For each comparable pair of sequence-similar on- and off-target sites in DNA, an ON:OFF ratio of the on-target cleavage yield versus the off-target cleavage yield is calculated by simple division. By contrast, a *specificity score* is calculated as the *odds ratio* of both yields. That is, if r_{on} and r_{off} are the average cleavage yields for the comparable on-target and off-target sites, respectively, then the specificity score S^{on}_{off} is defined as

$$S^{on}_{off} = \frac{r_{on}/(1-r_{on})}{r_{off}/\left(1-r_{off}\right)}$$

This formula is also suitable for evaluating specificity when measuring indel frequencies in CRISPR-treated cells, in which case r_{on} and r_{off} are the average indel frequencies at the on-target and off-target sites, respectively. The specificity score is symmetrical with respect to on-target and off-target cleavage and therefore can be a more informative metric when both are important. When the on-target cleavage rate is roughly constant, and the off-target rate is close to zero, the specificity score tracks the simple ON:OFF ratio, but it is more sensitive to changes in the on-target rate than the simple ratio assessment, as the latter is less sensitive to losses in cleavage activity.

RESULTS

Survey of MP modifications across the 20-nt guide sequence show specific sites that yield improved cleavage specificity

To improve the specificities of gRNAs for cognate protospacers, we envisioned a method that incorporates one or more chemical modifications in the ribose-phosphate backbone to alter the melting temperature (T_m) of the RNA-DNA duplex while maintaining the full complement of 20 nucleotides to discern cognate target sites in complex genomes. Examples of the chemical modifications we incorporated and examined in our studies are MP (Figure 1A) as well as 2′-*O*-methyl ('M'), 2′-*O*-methyl-3′-phosphorothioate ('MS') and 2′-*O*-methyl-3′-thiophosphonoacetate ('MSP') (Supplementary Figure S1). To help understand how these modifications can modulate RNA-DNA duplex stability in the context of gRNAs, we performed T_m studies using 20-nt RNA sequences containing up to nine identical modifications. Each RNA sequence was hybridized to a perfectly matched single-stranded oligodeoxynucleotide (ssODN) sequence to form a 20-bp duplex in which both strands further had non-complementary overhangs. We observed a progressive decrease of 1.0–1.3°C per MP and 1.3–1.5°C per MSP at physiological salt concentrations (Supplementary Figure S2), demonstrating that MP and MSP lower the stability of hybridization.

A

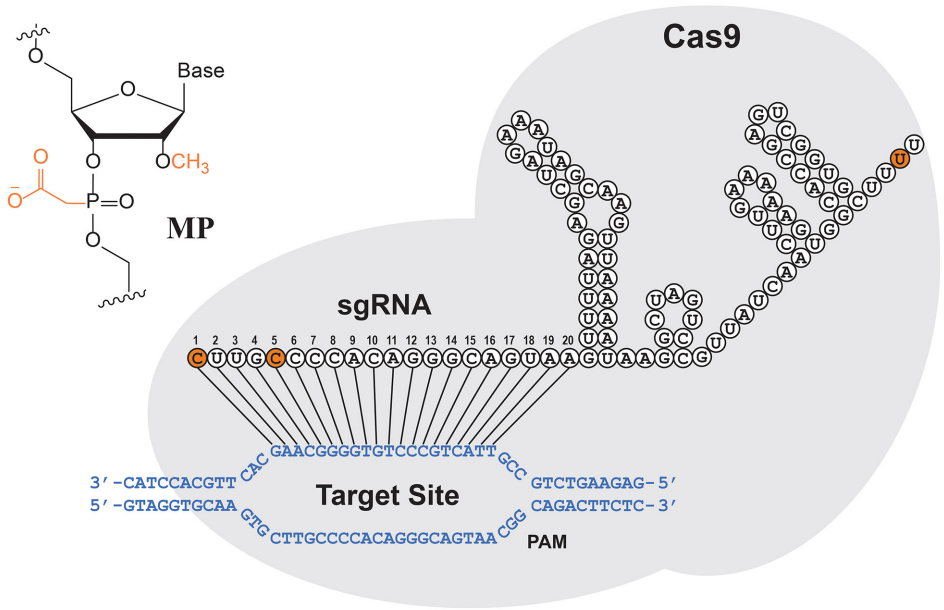

B

MP positions in 20-nt guide portion	Guide Sequence Portion	SPECIFICITY SCORES					
		CLTA4 ON:OFF1	CLTA4 ON:OFF2	CLTA4 ON:OFF3	HBB ON:OFF1	VEGFA ON:OFF2	IL2RG ON:OFF3
1	NNNNNNNNNNNNNNNNNNNN-	0.6	0.2	2.5	8.3	0.3	0.5
1,2	NNNNNNNNNNNNNNNNNNNN-	1.1	0.5	5.5	9.4	0.5	1.2
1,3	NNNNNNNNNNNNNNNNNNNN-	0.4	1.2	4.9	6.7	2.8	3.5
1,4	NNNNNNNNNNNNNNNNNNNN-	3.3	8.2	110	15	150	25
1,5	NNNNNNNNNNNNNNNNNNNN-	1.6	14	530	38	160	7.2
1,6	NNNNNNNNNNNNNNNNNNNN-	0.6	0.1	1.2	3.6	1.3	1.5
1,7	NNNNNNNNNNNNNNNNNNNN-	1.2	1.1	26	17	25	22
1,8	NNNNNNNNNNNNNNNNNNNN-	0.8	0.5	1.6	9.5	9.3	2.4
1,9	NNNNNNNNNNNNNNNNNNNN-	1.0	0.2	5.5	28	23	5.6
1,10	NNNNNNNNNNNNNNNNNNNN-	1.1	2.0	0.9	23	33	2.2
1,11	NNNNNNNNNNNNNNNNNNNN-	1.8	1.3	3.6	43	27	13
1,12	NNNNNNNNNNNNNNNNNNNN-	0.8	0.6	14	11	3.0	47
1,13	NNNNNNNNNNNNNNNNNNNN-	0.9	0.1	2.1	7.9	7.2	74
1,14	NNNNNNNNNNNNNNNNNNNN-	0.5	1.6	45	13	190	230
1,15	NNNNNNNNNNNNNNNNNNNN-	1.1	4.3	20	0.4	9.0	14
1,16	NNNNNNNNNNNNNNNNNNNN-	0.7	1.0	13	5.0	25	440
1,17	NNNNNNNNNNNNNNNNNNNN-	0.3	0.1	1.3	5.0	1.8	150
1,18	NNNNNNNNNNNNNNNNNNNN-	0.8	0.3	2.4	6.2	1.3	56
1,19	NNNNNNNNNNNNNNNNNNNN-	1.0	0.3	1.9	6.3	1.7	34
1,20	NNNNNNNNNNNNNNNNNNNN-	1.0	0.1	1.4	5.2	0.4	4.4

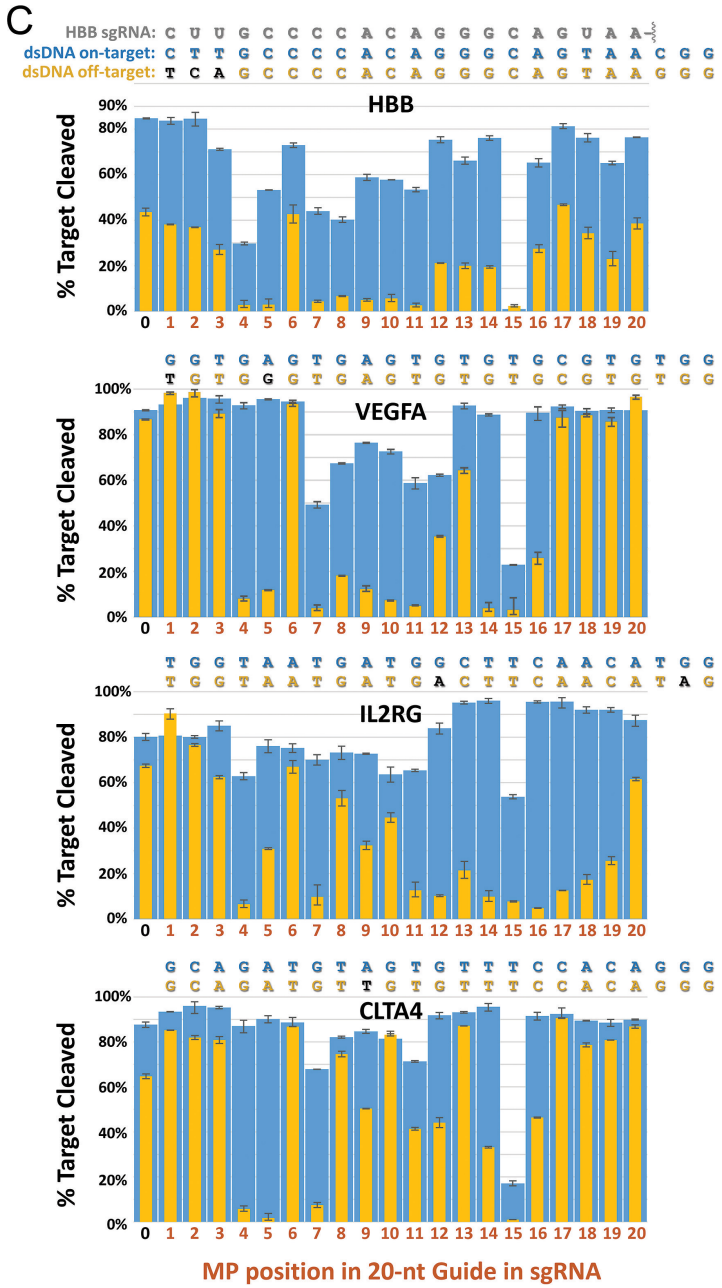

Figure 1. Chemically modified sgRNAs provide enhanced specificity of Cas9 cleavage *in vitro*. (**A**) Chemical structure of the MP modification (upper left inset). Schematic sequence and secondary structure of the HBB sgRNA loaded into Cas9 protein and bound to a complementary DNA target site in the *HBB* gene. Nucleotides with MP modification are indicated by orange circles for the representative example of HBB_5MP_1xMP sgRNA in which position 5 is MP-modified for specificity enhancement. The PAM sequence motif (-NRG-) required for DNA binding by Cas9 is marked. (**B**) For each DNA target sequence from *CLTA, HBB, VEGFA* and *IL2RG* genes, a series of sgRNAs was synthesized by sequentially walking an MP modification indicated by N across the complementary guide sequence while retaining MP modifications at the 5′ and 3′ ends of the sgRNAs ('1xMP' end protection to resist exonucleases). Each on- or off-target site was incorporated in a linear DNA construct subjected to *in vitro* cleavage (IVC) assays to measure cleavage yields for calculation of ON:OFF target cleavage ratios and specificity scores, all compiled in Supplementary Figure S3. A heat map of specificity scores indicates the relative specificity enhancement observed for each position in the MP walks (higher scores indicate higher on-target specificity). Magnitudes of specificity scores vary according to the on- & off-target sites compared per column as indicated; therefore, magnitudes should not be compared between columns. (**C**) Bar graphs show the on- and off-target cleavage activities used to calculate the specificity scores depicted in the heat map in (B). Blue and gold bars represent the average fraction ± S.D. of cleaved DNA containing the on-target site (blue) or off-target site (gold) measured in duplicate assays per sgRNA. IVC assay yields are shown for sgRNAs targeting the HBB, VEGFA, IL2RG and CLTA4 sites using sgRNPs containing no RNA modifications (indicated as 0 on the x-axis), an MP modification at both 5′ and 3′ termini of the sgRNA ('1xMP', indicated by 1 on the x-axis), or a single MP modification at positions 2–20 plus an MP modification at both RNA termini (1xMP end protection). sgRNA sequences can be found in Supplementary Table S1. Alignment between the 20-nt guide sequence portion of a representative sgRNA and its dsDNA target site and off-target site (both as in the human genome) is illustrated at top for the HBB target as an example. Sequences of dsDNA on- and off-target sites assayed for cleavage are displayed in blue and gold text, respectively, with mismatches in the off-target sites indicated in black lettering and with the PAM sequence motif (-NRG-) for each site shown on the far right. The on- and off-target sequences in each of the four panels are HBB ON & OFF1, VEGFA ON & OFF2, IL2RG ON & OFF3, and CLTA4 ON & OFF3, respectively (DNA sequences and genomic coordinates are presented in Table 1). Mean and S.D. values are listed in Supplementary Table S3.

Table 1. On- and off-target sequences incorporated in linear DNA constructs for IVC assays or as found naturally in human cells for targeting of *HBB*, *VEGFA* and *IL2RG* loci by CRISPR–Cas9 sgRNP

Target or Off-target Site Name	Sequence	Genomic Coordinates (in human reference genome *GRChg38*)
HBB ON	CTTGCCCCACAGGGCAGTAACGG	Chr11:5 226 968–5 226 990
HBB OFF1	tcaGCCCCACAGGGCAGTAAGGG	Chr9:101 833 584–101 833 606
HBB OFF5	gcTGCCCCACAGGGCAGcAAAGG	Chr12:124 319 282–124 319 304
HBB OFF9	aTTGCCCCACgGGGCAGTgACGG	Chr12:93 155 409–93 155 431
VEGFA ON	GGTGAGTGAGTGTGTGCGTGTGG	Chr6:43 769 717–43 769 739
VEGFA OFF2	tGTGgGTGAGTGTGTGCGTGAGG	Chr5:116 098 962–116 098 984
IL2RG ON	TGGTAATGATGGCTTCAACATGG	ChrX:71 111 519–71 111 541
IL2RG OFF2	TGGTgAgGATGGCTTCAACACGG	Chr1:167 730 172–167 730 194
IL2RG OFF3	TGGTAATGATGaCTTCAACATAG	Chr3:72 764 801–72 764 823
CLTA1 ON	AGTCCTCATCTCCCTCAAGCAGG	Chr9:36 211 735–36 211 757; Chr12:7 607 297–7 607 319
CLTA1 OFF1	AGTCCTCAaCTCCCTCAAGCAGG	Chr8:15 688 928–15 688 950
CLTA1 OFF3	AcTCCTCATCcCCCTCAAGCAGG	Chr15:88 845 439–88 845 461
CLTA4 ON	GCAGATGTAGTGTTTCCACAGGG	Chr9:36 211 782–36 211 804
CLTA4 OFF1	GCAGATGTAGTaTTTCCACAGGG	Artificial construct
CLTA4 OFF2	cCAGATGTAGcGTTTCCACAGGG	Artificial construct
CLTA4 OFF3	GCAGATGTtGTGTTTCCACAGGG	Artificial construct

The sequences of the CLTA4 off-target sites were artificially devised and were incorporated in DNA constructs for IVC assays.

Our initial screens for higher specificity employed an *in vitro* DNA cleavage (IVC) assay to explore modifications beyond the first three 5′ nucleotides in guide sequences. We found that one or two MP modifications at internal nucleotides in 20-nt guide sequences in sgRNAs could greatly improve specificity when incorporated at specific sites. To elucidate the impacts of MP's on CRISPR cleavage activities, we systematically walked a single MP across the guide sequences in sgRNAs for four different genes: *HBB, IL2RG*, *VEGFA* and C*LTA* (Figure 1B). We used an HBB guide reported by several groups to be highly efficient in editing the sickle cell disease (SCD) mutation; however, it is also known to cleave an off-target site (OFF1) on chromosome 9 with high efficiency (29–32) which could induce events such as translocations that might elicit unwanted effects. Likewise, the IL2RG and VEGFA target sequences in our studies were previously identified as useful for editing these clinically important genes (1,23).

We measured IVC activities for these three targets and another well-studied target (CLTA4) (3) by cleaving fragments of dsDNA containing a matching target sequence or a cleavable off-target sequence having 1–3 mismatches (Table 1). To stabilize our sgRNAs against degradation, each modified sgRNA also contained single MP's on both termini (5′ and 3′) to impede exonucleases ('1xMP' protection). For each comparable pair of sequence-similar on- and off-target sites in DNA, the on-target cleavage yield versus off-target cleavage yield was compared as a simple ratio (ON:OFF) to help assess specificity (Supplementary Figure S3). We further calculated an odds ratio to provide a specificity score which better accounts for any substantial attenuation of the on-target activity than the simple ratio does (as explained in the Methods). Strikingly, the incorporation of a single internal MP modification at certain positions in the guide sequences for the four different targets showed markedly reduced off-target cleavage activities compared to the unmodified and 1xMP-only controls while on-target cleavage yields were largely maintained (Figure 1C and Supplementary Table S3).

There were three main regions of the guide sequence in which chemical modifications appear to enhance specificity. First, an MP at position 4, 5 or 7 (i.e. the fourth, fifth or seventh nucleotide from the 5′ end of the sgRNA) consistently reduced off-target cleavage by an order of magnitude. As shown in Figure 1 and Supplementary Figure S3, these modifications elicited excellent specificity enhancements across the differently targeted guide sequences. Interestingly, these positions flank position 6 where MP modification had little or no impact on cleavage.

The next most useful region for boosting specificity was positions 9–12, located at the outer boundary of the seed sequence (33,34). The third region where MP incorporation enhanced specificity of some sgRNAs was adjacent to position 15, especially at positions 14 and 16, although enhancements were limited to a subset of the sgRNAs tested. It is interesting to note that MP modification at position 15 strongly inhibited cleavage at all four targets, showing ∼3–4-fold reduction in on-target cleavage for CLTA4 and VEGFA and undetectable cleavage for HBB. Our finding that position 15 is especially intolerant of MP modification is interesting in light of contacts between the *S. py.* Cas9 protein and the gRNA backbone at positions 15–16 where a conformational change occurs in tyrosine Y450 upon protospacer binding (33).

For each of the four targets tested, the decrease in cleavage efficiency caused by off-target mismatches (relative to on-target cleavage) and the separate decrease caused by an MP modification which enhances specificity (such as the impact of 5MP modification on on-target cleavage) are not additive: a specificity-enhancing MP modification suppresses the mismatched sequence more substantially than the matched sequence. This non-additivity suggests that conformational changes are likely important for the specificity enhancements observed (35,36).

We also tested 55 pairwise combinations of two internal MP's in the HBB guide and 36 pairwise combinations in the IL2RG guide using the IVC assay. As objective measures of the relative benefits of modifications at different positions in 20-nt guide sequences, we calculated both ON:OFF

cleavage ratios and specificity scores, the latter based on the odds ratio of the on- versus off-target cleavage yields in IVC assays as described above. The results compiled from MP walks and pairwise combinations of MP's in synthetic sgRNAs are shown in Supplementary Figures S3–S5. Although the sgRNAs with two internal MP's showed modestly improved specificity for cleaving HBB and IL2RG targets compared with sgRNAs containing a single internal MP, this came at the cost of reduced on-target activity, especially for the HBB target.

MP-modified sgRNAs enhance specificity of indel formation and editing of the sickle cell locus while maintaining high on-target performance in human cells

A subset of the MP-modified HBB sgRNAs were assayed in mobilized human peripheral blood CD34+ HSPCs in an effort to obtain higher specificity for cleaving the *HBB* gene as might benefit gene therapies for sickle cell disease (30–32). To explore the impacts of cell types and genetic backgrounds, we also performed assays using K562 cells and induced Pluripotent Stem (iPS) cells.

Results from targeted deep sequencing of indels at the HBB ON and OFF1 target sites are compiled in Supplementary Table S4, and a selection of these data comprising the best specificity enhancers are shown in Figure 2A. In all three cell types, we observed the greatest specificity enhancement when MP was incorporated at position 5 or 11, which reduced OFF1 cleavage in CD34+ cells from ∼50% to <2% while retaining high on-target activity. We also observed substantial improvements in specificity when MP was incorporated at position 7, 9 or 10, although to a lesser degree. In our cell-based assays, many of the sgRNAs containing two internal MP's gave markedly fewer off-target indels than sgRNAs containing a single internal MP, consistent with our IVC results; however, the internal MP pairs tended to reduce on-target indel frequencies more severely in cells than in the IVC assays (Supplementary Table S4).

We next tested the performance of chemically modified sgRNAs in HDR-mediated editing of the *HBB* gene. HBB sgRNA with an internal MP modification at position 5 or 11 was complexed with Cas9 protein, and the resulting sgRNP complex was transfected into K562 cells along with an ssODN donor DNA designed to edit the *HBB* gene by knocking-in the SCD mutation (31). We quantified the yields of edits and indels at the ON and OFF1 target sites using targeted deep sequencing (Figure 2B and Supplementary Table S5), and we observed ∼30–35% correctly edited alleles and a commensurate decrease in *HBB* indels when ssODN was co-transfected. Interestingly, we also observed ∼2% editing at the OFF1 site, in which the SCD mutation was inadvertently introduced at that locus when unmodified or 1xMP-modified sgRNP was co-transfected with the ssODN donor. This suggests that the donor, which has substantial sequence similarity to both sides of the cut site in OFF1 (as shown in Supplementary Figure S6), mediates an appreciable level of off-target editing. Cells treated with the ssODN donor plus the sgRNP modified at position 5 or 11 showed striking reductions in indel rates at OFF1 and, importantly, the HDR activity at OFF1 was reduced by ∼40–120 fold.

To more broadly assess genome-wide off-target activities of HBB sgRNPs in cells, we used a target enrichment library designed to capture 1-kb segments of genomic DNA (gDNA) centered on 959 potential off-target sites as well as the on-target site, aiming to capture all PAM-addressable loci in unmasked regions of the human genome with 5 or fewer mismatches relative to the 20-bp *HBB* target (all loci are listed in Supplementary Table S6). We performed deep sequencing of the 960 loci isolated from K562 cells after transfection with sgRNP containing either unmodified, 1xMP-modified, or 1xMP plus position 5 MP–modified sgRNA to measure the indel frequencies at the 960 loci (Supplementary Table S6). The modified and unmodified sgRNAs gave high indel rates at the *HBB* target site (∼84–85%), and the most active off-target site was HBB OFF1 as usual. Of the remaining 958 loci, only 3 (OFF5, OFF9 and OFF17) yielded indels at substantially higher rates than mock transfections lacking Cas9 sgRNP (i.e. the logarithm of odds ratio was >1), although the yields at the latter two loci were at or near the ∼0.1% detection limit in this experiment.

To achieve greater sensitivity in measuring the specificity of HBB guides containing an MP at position 5 or 11, we used targeted deep sequencing of PCR amplicons to quantify indels at the same 5 active on- and off-target loci plus another 14 potential off-target sites to collectively assay all PAM-addressable loci in unmasked regions of the human genome with 3 or fewer mismatches versus the 20-bp *HBB* target. Of the 18 potential off-target sites, only 3 showed indel frequencies significantly higher than the detection limits set by the mock transfections: OFF1, OFF5 and OFF9 (Supplementary Table S7). These off-target activities were substantially reduced when position 5 or 11 was MP modified, with position 11 showing somewhat better specificity (Figure 2C).

MP modification at select positions enhance specificity in sgRNAs targeting three different loci

Results from cell-based assays of synthetic IL2RG and VEGFA sgRNAs showed that MP modifications at specific positions markedly reduced off-target activities while maintaining high on-target activities (Figure 3A). In contrast to the HBB results, however, VEGFA and IL2RG sgRNAs containing MP modifications at the 5′ and 3′ termini (1xMP end protection) affected specificity more strongly, although the effects were divergent. For VEGFA, the 1xMP guide showed a notably higher rate of off-target indels than the unmodified guide, whereas the opposite was true for IL2RG as the 1xMP guide showed a lower rate of off-target indels than the unmodified guide. These results indicate that a single MP modification at the 5′ terminus can affect the specificity of some guides, perhaps depending on the locations of mismatches in the off-target sequences undergoing cleavage.

To further explore the specificity effects of one or more MP's at the 5′ end of a guide sequence, we synthesized HBB, VEGFA and CLTA4 sgRNAs incorporating from 1 to 5 consecutive MP's at their 5′ ends. These sgRNAs were evaluated in IVC assays, and each guide showed a successive attenuation of cleavage activity as MP modifications were added sequentially to its 5′ end (Supplementary Figure S7

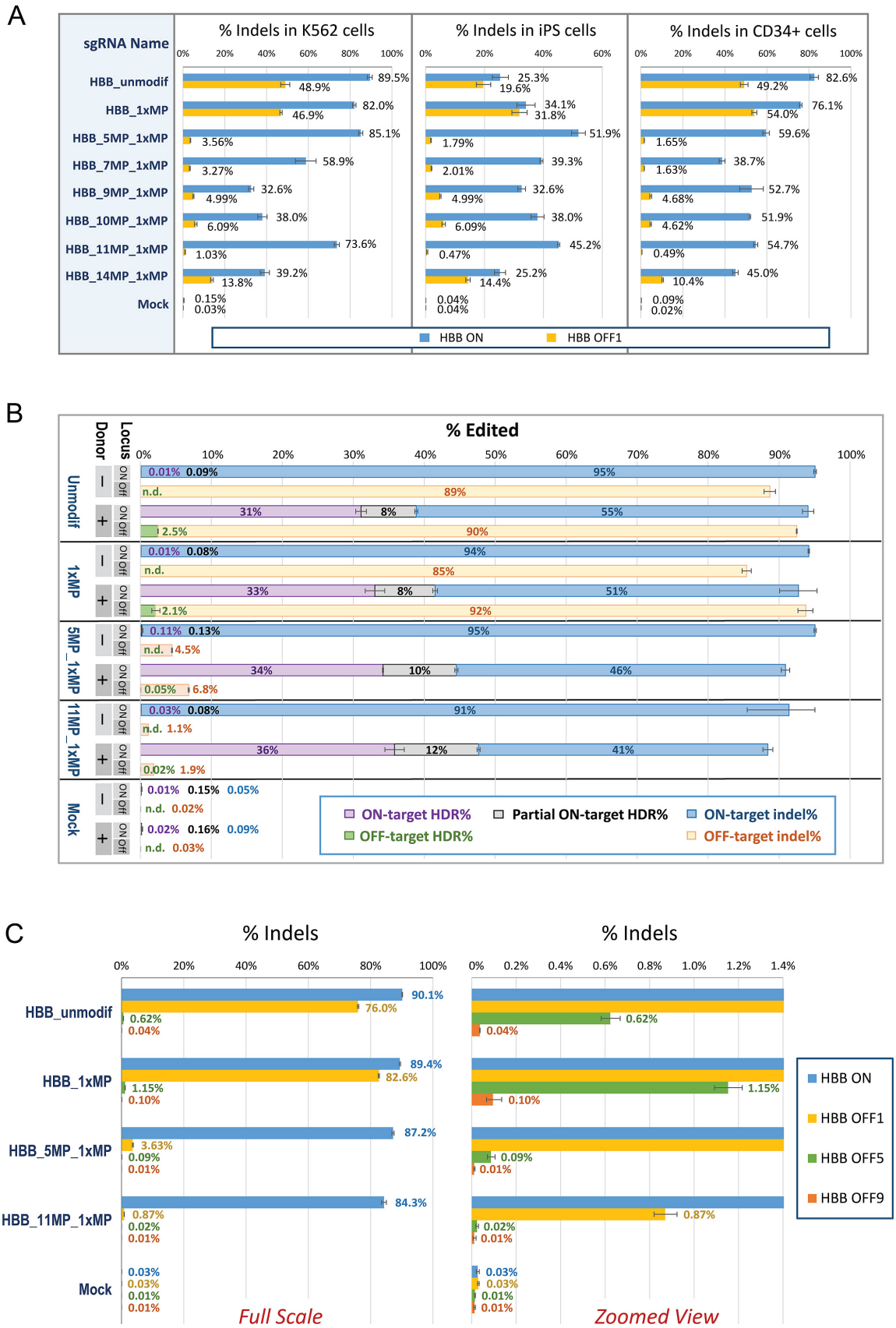

Figure 2. MP modification of select positions in synthetic sgRNAs targeting *HBB* enhances specificity of indel formation and editing of the sickle cell locus in human cells. (**A**) Gene disruption by mutagenic NHEJ as measured by deep sequencing of PCR amplicons of the HBB ON and OFF1 target

and Table S3). For the on- and off-target sites compared, the successive addition of 5′ terminal MP's improved specificities until a peak was reached at a certain number of MP's, beyond which further addition of MP's inhibited on-target cleavage activity. The number of successive 5′ MP modifications conferring the highest levels of specificity improvement was variable amongst the different targets, suggesting that the level of specificity enhancement attainable by this approach can strongly depend on the particular on- and off-target sequences involved.

In cell-based assays, adding an MP modification at position 5, 7 or 11 in 1xMP-modified IL2RG, VEGFA and HBB sgRNAs resulted in significant reductions in off-target activities for all three guides while on-target activities were largely maintained (Figure 3A). As we routinely observed rather low indel frequencies at the IL2RG OFF2 site, and this activity was further attenuated by 1xMP modification of the sgRNA, we performed transfections using a series of four increasing amounts of IL2RG sgRNP. The on-target activity observed was quite high in all cases, yielding increasing levels of indels as the sgRNP concentration was increased from 25 to 200 pmoles per 20 uL transfection. Even at the highest concentration tested, an MP modification at position 5 or 11 reduced the off-target indel frequency from ∼0.1% to less than our limit of detection, which we estimate to be ∼0.05% based on measurements of indels in the mock transfections lacking Cas9 sgRNP (Figure 3B).

DISCUSSION

In summary, we show that chemical modifications of the ribose-phosphate backbone of sgRNAs at specific positions in their 20-nt guide sequences can markedly reduce the frequency of off-target indels and HDR misediting by CRISPR–Cas9 in cells, without sacrificing on-target activity. Cas9-guided cleavage involves interactions between Cas9 protein and guide RNA and subsequently between the complexed Cas9 gRNP and a complementary DNA locus via a multi-step process involving conformational rearrangements (37,38). A general strategy for improving the specificity of Cas9-guided cleavage is to lower the overall free-energy barrier between formation and dissociation of the gRNP:DNA complex, and/or to increase the overall free-energy barrier between the ground-state complex and its transition state for cleavage (39). Our T_m results show that MP modifications in guide sequences destabilize proximal base pairing, and this could impact the dynamics of hybridization of a guide sequence as it interrogates corresponding on- and off-target sites. Furthermore, given the extensive interactions between the gRNA and Cas9 observed in structural studies, MP modifications could perturb RNA-protein interactions in gRNP:DNA complexes which might affect one or more thermodynamic barriers that modulate specificity.

Recent structure-function studies of Cas9 provide clues to why MP modifications at or near positions 5 and 11 are especially effective at improving specificity. Position 11 lies at the boundary of the 10-nt seed region of the gRNA which is preorganized into an A-form helical conformation by Cas9 binding. Subsequent binding of the Cas9 gRNP to a cognate PAM and complementary protospacer results in local DNA melting, RNA strand invasion and stepwise conformational changes to achieve R-loop formation and cleavage of the DNA target site (37,40). When the seed sequence is sufficiently complementary to a target site, hybridization proceeds through the seed sequence into the non-seed portion of the guide sequence until a conformational gate or checkpoint is reached for cleavage (40,41). At this checkpoint, five clusters of amino acids (Clusters 1−5) in the REC3 domain of Cas9 are thought to interact directly with the RNA-DNA helix at its PAM-distal region to monitor whether it forms a proper pseudo-A-form helical structure (16). In models of the REC3 domain engaged in proofreading this structure, the ribose-phosphate backbone at position 11 in the gRNA interacts with Cluster 5 in REC3, and the backbone of the DNA nucleotide that hybridizes to position 11 interacts with Cluster 3 [(16), see their Figure 3A]. As such, an MP modification at position 11 could weaken the interaction with the REC3 domain and raise the energy barrier of the last conformational gate to cleavage and might also increase the off rate (k_{off}) of Cas9 gRNP binding to complementary genomic sites. Either or both effects would raise the stringency of hybridization for a correct match. In assays of the HBB OFF1 locus where off-target mismatches lie entirely at the PAM-distal end, an MP modification at position 11 in HBB sgRNA may shift the binding equilibrium of REC3 away from its PAM-distal−bound state at the checkpoint and thus inhibit cleavage, especially when the PAM-distal region contains mismatches.

Likewise, the ribose-phosphate backbone at position 5 in the gRNA interacts with Clusters 1 and 3 in the REC3 domain, and the backbone of the DNA nucleotide that hybridizes to position 5 interacts with Cluster 2, suggesting

←

sites in K562 cells, induced pluripotent stem cells (iPSCs), and CD34+ hematopoietic stem and progenitor cells (HSPCs) induced by transfection of Cas9 protein complexed with unmodified or modified synthetic sgRNA. Mock transfections are minus Cas9 sgRNP. Bars represent average values ± S.D., $n = 3$. Results from IVC assays of the same set of sgRNAs are shown in the right panel as average values ± S.D., $n = 2$. (**B**) Editing of the sickle cell disease (SCD) locus in K562 cells induced by transfection of Cas9 protein complexed with unmodified or modified sgRNA and co-transfection of a single-stranded oligonucleotide (ssODN) donor DNA designed to knock in the SCD point mutation and a synonymous mutation in the SCD codon as well as a PAM-silencing mutation, as shown in Supplementary Figure S6. The frequency of indels and edits at the ON and OFF1 target sites were quantified by deep sequencing of PCR amplicons, and average values ± S.D. from triplicate transfections are plotted in stacked bars. The frequencies of indels are plotted in blue and gold bars for the on- and off-target sites, respectively. Complete and partial HDR frequencies (the latter indicated by sequencing reads showing the PAM-silencing mutation as the only change) are plotted in purple and gray bars respectively for on-target editing. We also detected a low level of HDR editing at the off-target locus in the presence of ssODN donor as plotted in green bars. Measured values are labeled on the bars in matching colors as indicated in the legend (n.d. = none detected). Mean and S.D. values are tabulated in Supplementary Table S5. (**C**) Indel frequencies at three HBB off-target loci (of 18 assayed) which showed detectable cleavage by deep sequencing of PCR amplicons generated from K562 cells after transfection with Cas9 protein complexed with unmodified or modified sgRNA. Mock transfections are minus Cas9 sgRNP. Bars represent average values ± S.D., $n = 3$. Data from all 18 loci assayed are shown in Supplementary Table S7.

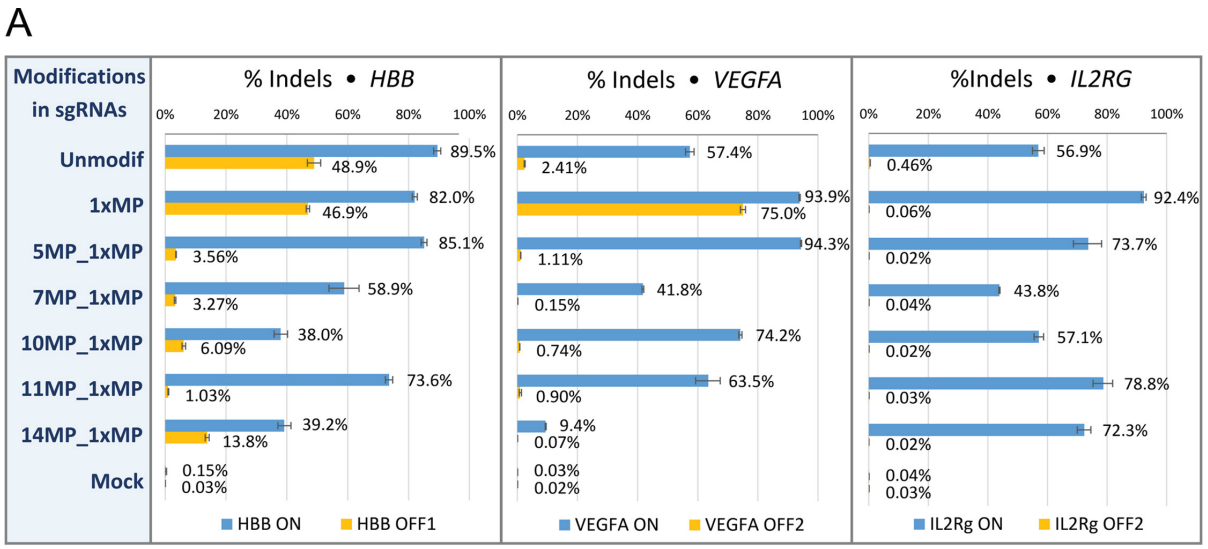

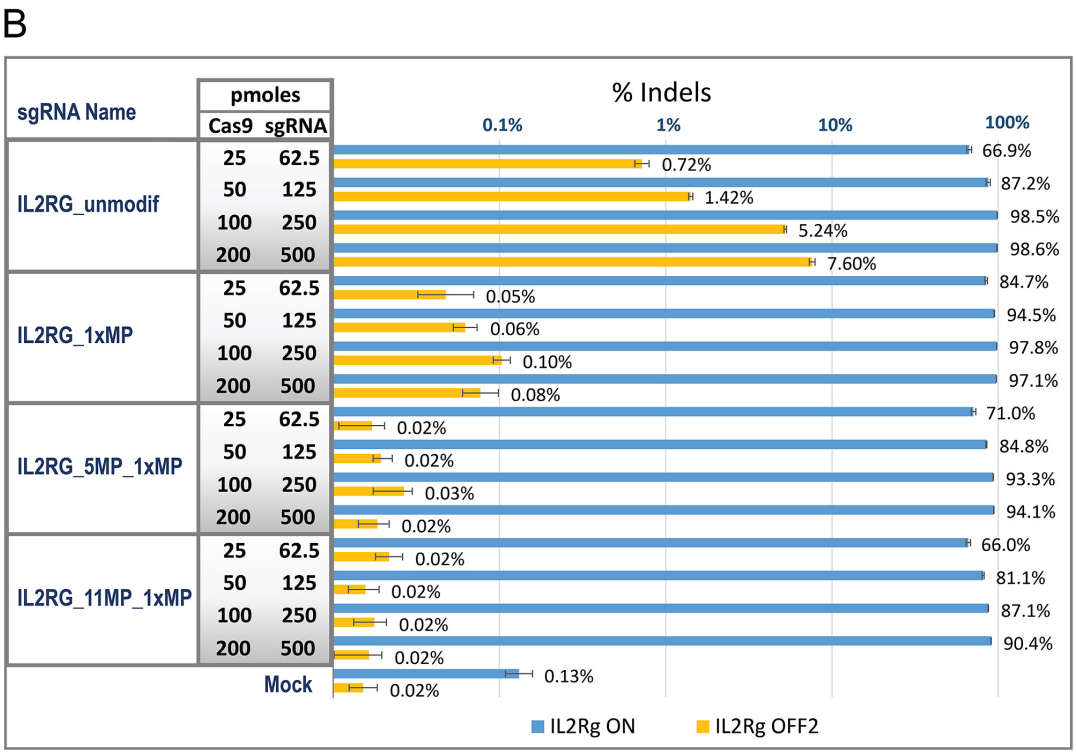

Figure 3. MP modification of select positions in synthetic sgRNAs targeting *VEGFA* and *IL2RG* enhances specificity in human cells. (**A**) Gene disruption by mutagenic NHEJ as measured by deep sequencing of PCR amplicons of the ON and OFF2 target sites for VEGFA as well as the ON and OFF2 target sites for IL2RG in K562 cells after transfection with Cas9 protein complexed with unmodified or modified synthetic sgRNA. Bars represent average values ± S.D., $n = 3$. For comparison, the results from assays of HBB ON and OFF1 target sites are redisplayed as shown in Figure 2A. (**B**) Indel frequencies (on logarithmic scale) at the IL2RG ON and OFF2 target sites in K562 cells transfected with an increasing concentration of sgRNA:Cas9 protein complex, as measured by deep sequencing of PCR amplicons of both loci. Bars represent average values ± S.D., $n = 3$. Mock transfections are minus Cas9 sgRNP. Detection limit is ∼0.05% based on the levels of indels measured in mock transfections.

that the specificity improvements we observe for MP modification at position 5 could modulate progression through the last conformational gate to the active state for cleavage. Future structure-function studies using modified sgRNAs as described here could help illuminate the molecular mechanisms controlling specificity enhancement and, in turn, advance our understanding of the mechanisms governing CRISPR–Cas binding and/or cleavage.

Chemical synthesis can provide robust methods for scalable manufacturing of highly pure sgRNAs and affords unique opportunities for sgRNA design and precise installation of molecular functionality to enhance CRISPR–Cas performance in profoundly useful ways, as demonstrated here for specificity. Incorporating modifications such as MP and MSP in the ribose-phosphate backbone of guide sequences allows users to tailor specificity to select targets, to cellular environments and perhaps to some other CRISPR systems, such as Cpf1 (42). This method provides a versatile tool for enhancing specificity alongside methods that limit the duration of CRISPR–Cas exposure or that employ high-fidelity Cas protein variants. Future studies could investigate whether combinations of chemically modified sgRNAs and high-fidelity Cas variants might yield even further improvements in specificity and might also enable more flexible control of delivery and activity in different types of cells and tissues. In conclusion, this study demonstrates that chemical modifications at specific sites in guide sequences can dramatically improve the specificity and flexibility of CRISPR–Cas systems for precise editing of genes and genomes.

AVAILABILITY

The human reference genome *GRChg38* is accessible online on the UCSC Human Genome Browser (http://genome.ucsc.edu/).

SUPPLEMENTARY DATA

Supplementary Data are available at NAR Online.

ACKNOWLEDGEMENTS

We thank P. Kirby for assistance with RNA synthesis, J. Swan for assistance with developing RNA purification, L. Monfregola for assistance with T_m measurements, P. Tsang for assistance in designing the SureSelect library, and Q. Wang for assistance with statistical methods. We are grateful to J. Myerson for intellectual contributions, and B. Peter and S. Laderman for critical reading of the manuscript. C. Carstens, R. Kaiser, A. Tsalenko and members of Agilent Research Laboratories provided helpful input, comments and discussion.

FUNDING

Funding for open access charge: Agilent Technologies.

Conflict of interest statement. D.E.R., D.T., I.S., S.M.P., B.D.L., C.W.Y., B.C., J.R.S, L.B. and D.J.D. are employees of Agilent Technologies. In addition, one of these authors individually owns patent rights for one of the chemical modifications used in this research.

REFERENCES

1. Fu,Y., Foden,J.A., Khayter,C., Maeder,M.L., Reyon,D., Joung,J.K. and Sander,J.D. (2013) High-frequency off-target mutagenesis induced by CRISPR–Cas nucleases in human cells. *Nat. Biotechnol.*, **31**, 822–826.
2. Hsu,P.D., Scott,D.A., Weinstein,J.A., Ran,F.A., Konermann,S., Agarwala,V., Li,Y., Fine,E.J., Wu,X., Shalem,O. *et al.* (2013) DNA targeting specificity of RNA-guided Cas9 nucleases. *Nat. Biotechnol.*, **31**, 827–832.
3. Pattanayak,V., Lin,S., Guilinger,J.P., Ma,E., Doudna,J.A. and Liu,D.R. (2013) High-throughput profiling of off-target DNA cleavage reveals RNA-programmed Cas9 nuclease specificity. *Nat. Biotechnol.*, **31**, 839–843.
4. Tsai,S.Q. and Joung,J.K. (2016) Defining and improving the genome-wide specificities of CRISPR–Cas9 nucleases. *Nat. Rev. Genet.*, **17**, 300–312.
5. Zischewski,J., Fischer,R. and Bortesi,L. (2017) Detection of on-target and off-target mutations generated by CRISPR/Cas9 and other sequence-specific nucleases. *Biotechnol. Adv.*, **35**, 95–104.
6. National Academy of Sciences (2017) *Human Genome Editing: Science, Ethics, and Governance*. The National Academies Press, Washington, DC.
7. Reimer,J., Knoess,S., Labuhn,M., Charpentier,E.M., Gohring,G., Schlegelberger,B., Klusmann,J.H. and Heckl,D. (2017) CRISPR–Cas9-induced t(11;19)/MLL-ENL translocations initiate leukemia in human hematopoietic progenitor cells in vivo. *Haematologica*, **102**, 1558–1566.
8. Tycko,J., Myer,V.E. and Hsu,P.D. (2016) Methods for optimizing CRISPR–Cas9 genome editing specificity. *Mol. Cell*, **63**, 355–370.
9. Fu,Y., Sander,J.D., Reyon,D., Cascio,V.M. and Joung,J.K. (2014) Improving CRISPR–Cas nuclease specificity using truncated guide RNAs. *Nat. Biotechnol.*, **32**, 279–284.
10. Kim,D., Bae,S., Park,J., Kim,E., Kim,S., Yu,H.R., Hwang,J., Kim,J.I. and Kim,J.S. (2015) Digenome-seq: genome-wide profiling of CRISPR–Cas9 off-target effects in human cells. *Nat. Methods*, **12**, 237–243.
11. Ran,F.A., Hsu,P.D., Lin,C.Y., Gootenberg,J.S., Konermann,S., Trevino,A.E., Scott,D.A., Inoue,A., Matoba,S., Zhang,Y. *et al.* (2013) Double nicking by RNA-guided CRISPR Cas9 for enhanced genome editing specificity. *Cell*, **154**, 1380–1389.
12. Tsai,S.Q., Wyvekens,N., Khayter,C., Foden,J.A., Thapar,V., Reyon,D., Goodwin,M.J., Aryee,M.J. and Joung,J.K. (2014) Dimeric CRISPR RNA-guided FokI nucleases for highly specific genome editing. *Nat. Biotechnol.*, **32**, 569–576.
13. Guilinger,J.P., Thompson,D.B. and Liu,D.R. (2014) Fusion of catalytically inactive Cas9 to FokI nuclease improves the specificity of genome modification. *Nat. Biotechnol.*, **32**, 577–582.
14. Kleinstiver,B.P., Pattanayak,V., Prew,M.S., Tsai,S.Q., Nguyen,N.T., Zheng,Z. and Joung,J.K. (2016) High-fidelity CRISPR–Cas9 nucleases with no detectable genome-wide off-target effects. *Nature*, **529**, 490–495.
15. Slaymaker,I.M., Gao,L., Zetsche,B., Scott,D.A., Yan,W.X. and Zhang,F. (2016) Rationally engineered Cas9 nucleases with improved specificity. *Science*, **351**, 84–88.
16. Chen,J.S., Dagdas,Y.S., Kleinstiver,B.P., Welch,M.M., Sousa,A.A., Harrington,L.B., Sternberg,S.H., Joung,J.K., Yildiz,A. and Doudna,J.A. (2017) Enhanced proofreading governs CRISPR–Cas9 targeting accuracy. *Nature*, **550**, 407–410.
17. Kim,S., Kim,D., Cho,S.W., Kim,J. and Kim,J.S. (2014) Highly efficient RNA-guided genome editing in human cells via delivery of purified Cas9 ribonucleoproteins. *Genome Res.*, **24**, 1012–1019.
18. Zuris,J.A., Thompson,D.B., Shu,Y., Guilinger,J.P., Bessen,J.L., Hu,J.H., Maeder,M.L., Joung,J.K., Chen,Z.Y. and Liu,D.R. (2015) Cationic lipid-mediated delivery of proteins enables efficient protein-based genome editing in vitro and in vivo. *Nat. Biotechnol.*, **33**, 73–80.
19. Zetsche,B., Volz,S.E. and Zhang,F. (2015) A split-Cas9 architecture for inducible genome editing and transcription modulation. *Nat. Biotechnol.*, **33**, 139–142.
20. Petris,G., Casini,A., Montagna,C., Lorenzin,F., Prandi,D., Romanel,A., Zasso,J., Conti,L., Demichelis,F. and Cereseto,A. (2017) Hit and go CAS9 delivered through a lentiviral based self-limiting circuit. *Nat. Commun.*, **8**, 15334.

21. Shin,J., Jiang,F., Liu,J.J., Bray,N.L., Rauch,B.J., Baik,S.H., Nogales,E., Bondy-Denomy,J., Corn,J.E. and Doudna,J.A. (2017) Disabling Cas9 by an anti-CRISPR DNA mimic. *Sci. Adv.*, **3**, e1701620.
22. Dellinger,D.J., Timar,Z., Myerson,J., Sierzchala,A.B., Turner,J., Ferreira,F., Kupihar,Z., Dellinger,G., Hill,K.W., Powell,J.A. *et al.* (2011) Streamlined process for the chemical synthesis of RNA using 2'-O-thionocarbamate-protected nucleoside phosphoramidites in the solid phase. *J. Am. Chem. Soc.*, **133**, 11540–11556.
23. Hendel,A., Bak,R.O., Clark,J.T., Kennedy,A.B., Ryan,D.E., Roy,S., Steinfeld,I., Lunstad,B.D., Kaiser,R.J., Wilkens,A.B. *et al.* (2015) Chemically modified guide RNAs enhance CRISPR–Cas genome editing in human primary cells. *Nat. Biotechnol.*, **33**, 985–989.
24. Rahdar,M., McMahon,M.A., Prakash,T.P., Swayze,E.E., Bennett,C.F. and Cleveland,D.W. (2015) Synthetic CRISPR RNA-Cas9-guided genome editing in human cells. *Proc. Natl. Acad. Sci. U.S.A.*, **112**, E7110–E7117.
25. Kelley,M.L., Strezoska,Z., He,K., Vermeulen,A. and Smith,A. (2016) Versatility of chemically synthesized guide RNAs for CRISPR–Cas9 genome editing. *J. Biotechnol.*, **233**, 74–83.
26. Jacobi,A.M., Rettig,G.R., Turk,R., Collingwood,M.A., Zeiner,S.A., Quadros,R.M., Harms,D.W., Bonthuis,P.J., Gregg,C., Ohtsuka,M. *et al.* (2017) Simplified CRISPR tools for efficient genome editing and streamlined protocols for their delivery into mammalian cells and mouse zygotes. *Methods*, **121–122**, 16–28.
27. Lee,K., Mackley,V.A., Rao,A., Chong,A.T., Dewitt,M.A., Corn,J.E. and Murthy,N. (2017) Synthetically modified guide RNA and donor DNA are a versatile platform for CRISPR–Cas9 engineering. *Elife*, **6**, e25312.
28. Threlfall,R.N., Torres,A.G., Krivenko,A., Gait,M.J. and Caruthers,M.H. (2012) Synthesis and biological activity of phosphonoacetate– and thiophosphonoacetate–modified 2′-*O*-methyl oligoribonucleotides. *Org. Biomol. Chem.*, **10**, 746–754.
29. Cradick,T.J., Fine,E.J., Antico,C.J. and Bao,G. (2013) CRISPR/Cas9 systems targeting beta-globin and CCR5 genes have substantial off-target activity. *Nucleic Acids Res.*, **41**, 9584–9592.
30. Cavazzana,M., Antoniani,C. and Miccio,A. (2017) Gene Therapy for beta-Hemoglobinopathies. *Mol. Ther.*, **25**, 1142–1154.
31. DeWitt,M.A., Magis,W., Bray,N.L., Wang,T., Berman,J.R., Urbinati,F., Heo,S.J., Mitros,T., Munoz,D.P., Boffelli,D. *et al.* (2016) Selection-free genome editing of the sickle mutation in human adult hematopoietic stem/progenitor cells. *Sci. Transl. Med.*, **8**, 360ra134.
32. Dever,D.P., Bak,R.O., Reinisch,A., Camarena,J., Washington,G., Nicolas,C.E., Pavel-Dinu,M., Saxena,N., Wilkens,A.B., Mantri,S. *et al.* (2016) CRISPR/Cas9 beta-globin gene targeting in human haematopoietic stem cells. *Nature*, **539**, 384–389.
33. Jiang,F., Zhou,K., Ma,L., Gressel,S. and Doudna,J.A. (2015) A Cas9-guide RNA complex preorganized for target DNA recognition. *Science*, **348**, 1477–1481.
34. Semenova,E., Jore,M.M., Datsenko,K.A., Semenova,A., Westra,E.R., Wanner,B., van der Oost,J., Brouns,S.J. and Severinov,K. (2011) Interference by clustered regularly interspaced short palindromic repeat (CRISPR) RNA is governed by a seed sequence. *Proc. Natl. Acad. Sci. U.S.A.*, **108**, 10098–10103.
35. Wells,J.A. (1990) Additivity of mutational effects in proteins. *Biochemistry*, **29**, 8509–8517.
36. Kraut,D.A., Carroll,K.S. and Herschlag,D. (2003) Challenges in enzyme mechanism and energetics. *Annu. Rev. Biochem.*, **72**, 517–571.
37. Jiang,F. and Doudna,J.A. (2017) CRISPR–Cas9 structures and mechanisms. *Annu. Rev. Biophys.*, **46**, 505–529.
38. Sternberg,S.H., LaFrance,B., Kaplan,M. and Doudna,J.A. (2015) Conformational control of DNA target cleavage by CRISPR–Cas9. *Nature*, **527**, 110–113.
39. Bisaria,N., Jarmoskaite,I. and Herschlag,D. (2017) Lessons from Enzyme Kinetics Reveal Specificity Principles for RNA-Guided Nucleases in RNA Interference and CRISPR-Based Genome Editing. *Cell Syst.*, **4**, 21–29.
40. Dagdas,Y.S., Chen,J.S., Sternberg,S.H., Doudna,J.A. and Yildiz,A. (2017) A conformational checkpoint between DNA binding and cleavage by CRISPR–Cas9. *Sci. Adv.*, **3**, eaao0027.
41. Josephs,E.A., Kocak,D.D., Fitzgibbon,C.J., McMenemy,J., Gersbach,C.A. and Marszalek,P.E. (2015) Structure and specificity of the RNA-guided endonuclease Cas9 during DNA interrogation, target binding and cleavage. *Nucleic Acids Res.*, **43**, 8924–8941.
42. Zetsche,B., Gootenberg,J.S., Abudayyeh,O.O., Slaymaker,I.M., Makarova,K.S., Essletzbichler,P., Volz,S.E., Joung,J., van der Oost,J., Regev,A. *et al.* (2015) Cpf1 is a single RNA-guided endonuclease of a class 2 CRISPR–Cas system. *Cell*, **163**, 759–771.